# Journal of Applied Sciences

ISSN 1812-5654

science alert

ANSInet
an open access publisher
http://ansinet.com

Journal of Applied Sciences 13 (21): 4688-4694, 2013
ISSN 1812-5654 / DOI: 10.3923/jas.2013.4688.4694


# 3D Finite Element Analysis of a Single Asperity Tangential Elastic-plastic Deformation Characteristics

[1,2]Li Wang and [1,2]Yang Xiang
[1]School of Power and Engineering, Wuhan University of Technology, China
[2]Key Laboratory of Marine Power Engineering and Technology, Ministry of Communication, China

**Abstract:** This study is focus on the tangential contact characteristics of a single hemispherical asperity when the asperity deformed in the stages of normal elastic-plastic deformation by the finite element method. The normal elastic-plastic contact characteristics of a single asperity contacted with a rigid flat has been studied by some researchers, but the tangential contact characteristics of them is still missing in the detail. The single asperity finite element model is a 3D finite element solid model in the study of the tangential contact characteristics, it is different the plane finite element model in the study of the normal contact characteristics. The local mesh refinement method is applied to mesh the asperity model, within the elastic deformation of the asperity, the normal contact load and area in the finite element analysis have been compared with the Hertz contact theory, the difference is less than 5%, the asperity 3D finite element model has been verified. For tangential contact analysis, a normal displacement is applied at the pilot node of the rigid flat, the asperity will deformation from the elastic to plastic range. Then hold the deformation state, a tangential force is again applied to the pilot node , the rigid flat will move on the surface of the asperity in the range of the micro-displacement state. Under the different normal displacement, the results shows that linear relationship can be obtained between tangential force and tangential micro-displacement, in the range of about $0 \le \frac{\omega}{\omega_e} \le 70$ , tangent modulus has not obviously effect on the tangential contact stiffness; In the range of about $\frac{\omega}{\omega_e} > 70$ ,tangential contact stiffness increasing with the tangent modulus increasing.

**Key words:** Single asperity, tangential contact, strain hardening, elastic-plastic contact

## INTRODUCTION

Almost all of the machining surfaces are rough surfaces under microscopic scale; there are many tiny asperities on the machined surface. When two machined surfaces are squeezed in the external force, the actual contact is the contact between the asperities on the two machining plane, the actual contact area is only a small part of the nominal contact area. In the theoretical analysis, it has been proposed that contact of two roughness surfaces can be represented by an equivalent roughness surface in normal contact with a rigid flat. For the description of the asperities on the rough surface, GW model developed in (Greenwood and Williamson, 1966) described an statistical model based asperity to study contact between nominally flat surfaces, in GW model , a rough surface is represented by a large number of spherical asperities with constant radius of curvature and normal height distribution. An elastic-plastic micro-contact model was proposed on the basis of the volume conservation of plastically deformed asperities in (Chang *et al*., 1987). Recently, in order to consider the continuity and smoothness of variables across different stages of deformation, a improved model was proposed in (Zhao *et al*., 2000).The more accurate model (Kogut and Etsion, 2002) (KE model) was first proposed through the result of elastic-plastic contact of a hemisphere and a rigid flat using Finite Element Method (FEM) to study the evaluation of the plastic zone under frictionless contact condition. The relationship between the normal and tangential force-displacement was studied in (Vu-Quoc *et al*., 2001) for frictional elastic-plastic contact between two deformable spheres with FEM. A new meshed method of the deformable sphere was proposed in (Lin and Lin, 2006) to study the elastic-plastic contact analysis. The strain hardening effect was studied in (Sahoo *et al*., 2010) on the deformable sphere, The friction effect was studied in (Wang and Xiang, 2013) on the normal contact area and contact load, The effect was studied on the valve pressure drop for rough surface in (Jia *et al*., 2012), A 3D elastic frictional contact analysis was investigated between a cylinder and a flat surface in (Chen, 2012).

**Corresponding Author:** Li Wang, School of Power and Engineering, Wuhan University of Technology, China

Although many scholars have studied the single asperity normal elastic-plastic deformation process, this paper is focus on the tangential contact characteristics when the asperity in the stages of normal elastic-plastic deformation.

## THEORETICAL BACKGROUND

The contact of a deformable hemisphere and a rigid flat is shown in Fig. 1 where the dashed and solid lines represent the situation before and after contact respectively of the sphere of radius R. The figure also shows the interference $\omega$ and the contact radius r corresponding to a contact load P.

According to the Hertz contact theory (Timoshenko and Goodier, 1951), the critical interference, $\omega_c$, the marks of the transition from the elastic to the elastic-plastic deformation regime is given by:

$$\omega_c = (\frac{\pi KH}{2E})^2 R \tag{1}$$

The hardness, H, of the sphere is related to its yield strength, $\sigma_y$, by:

$$H = 2.8\ \sigma_y \tag{2}$$

The hardness coefficient, K, is related to the Poisson ratio, v, of the sphere by:

$$K = 0.454+0.41v \tag{3}$$

E is the Hertz elastic modulus defined as:

$$\frac{1}{E} = \frac{1-v_1^2}{E_1} + \frac{1-v_2^2}{E_2} \tag{4}$$

where, $E_1$, $E_2$ and $v_1$, $v_2$ are Young's modulus and Poisson's ratios of the two materials ,respectively. In the case of the rigid flat $E2\rightarrow\infty$.

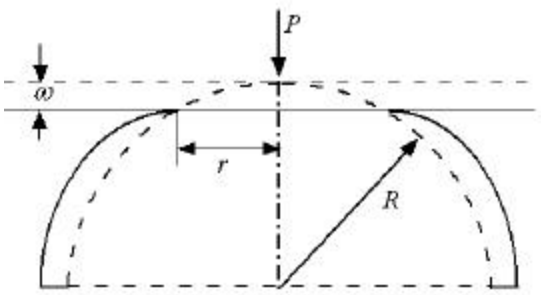


Fig. 1: A Deformable hemisphere asperity pressed by a rigid flat

for $\omega \le \omega_c$, the Hertz solution for elastic contact of a sphere and a rigid flat gives the contact load $P_e$ and the contact area $A_e$:

$$P_e = \frac{4}{3} E R^{1/2} \omega^{3/2} = P_c (\frac{\omega}{\omega_c})^{3/2} \tag{5}$$

$$A_e = \pi R \omega = A_c \frac{\omega}{\omega_c} \tag{6}$$

where, $P_c$ and $A_c$ are the contact load and contact area ,respectively at $\omega = \omega_c$. $P_e$ and $A_e$ can be normalized by $P_c$ and $A_c$, respectively, to obtain simple exponential functions of dimensionless interference, $\omega/\omega_c$, These functions are independent of the material properties and sphere radius.

The critical normal contact stiffness is defined as:

$$K_c = \frac{P_c}{\omega_c} \tag{7}$$

**Finite element model:** The contact of deformable hemisphere asperity with a rigid flat is modeled using the finite element software ANSYS.A hemisphere asperity was generated by rotating a quarter circle areas about an axis. The mesh of the quarter circle area was divided into two stages, In the first stage, the mesh of the quarter circle area was partitioned two region with different mesh density. In the region within the spherical vertex as the center of the circle, 0.1R as the radius has been meshed with fine mesh density; the remainder of the quarter circle has been meshed with coarser mesh density. The finite element model of the quarter circle in the first stage was shown in the Fig. 4a. In the second stages, the nodes and the elements of the finite element model shown in Fig.4.a in the potential contact surfaces within the 0.1R area was meshed by the ANSYS unique local mesh refinement method. The final finite element model of the quarter circle was shown in the Fig. 4b. Because the quarter circle was set as the cross-section of the three-dimension single asperity finite element model, it was meshed by the MESH200 element. Due to the advantage of simulation of symmetric problems, then the meshed area was rotated 180 degrees about its axis to get the finite element model of the single asperity which is SOLID185 element. The flat contacted with the asperity was represented by a area, In the ANSYS, the flat was meshed as a rigid target surface with a pilot node. The external load was applied through the pilot node.

During the quarter circle meshing, local mesh refinement method was applied to refine the potential contact area nodes. There are different mesh refinement

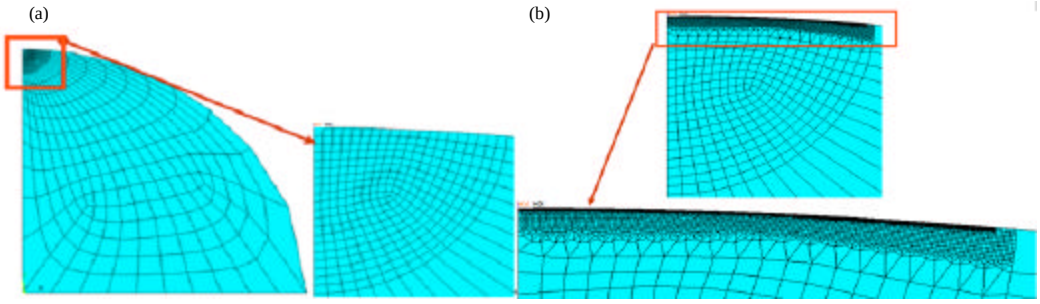


Fig. 2(a-b): The finite element model of the quarter circle (a) Initial mesh and (b) Local mesh refinement

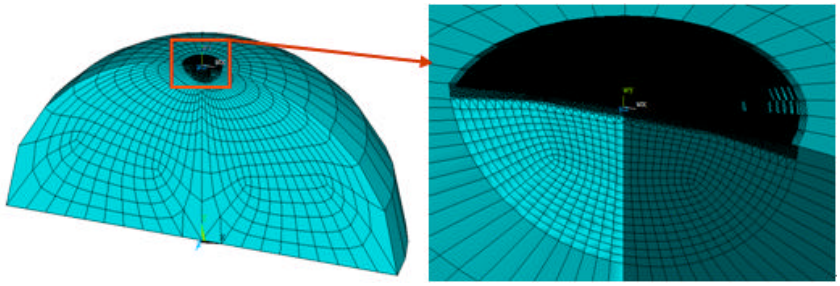

Fig. 3: The finite element model of a single asperity

levels in ANSYS; each refinement level has different mesh density, LEVEL from 1 to 5 attempts to provide gradually decreasing element edge lengths. In order to investigate the effect of mesh size on the solutions of contact parameters, six kinds of mesh refinement were provided in the present to compare their solution with the Hertz theoretical solutions, which were available only in elastic regime without frictionless.

In the elastic deformation analysis of the single asperity, the option of static small displacement in the ANSYS was adopted for the calculations in the elastic regime. Targe170 element and CONTA174 element were set as the "target " element and "contact" element , respectively. In the contact analysis, the rigid flat was controlled by creating a pilot node ,load boundary condition was applied by the pilot node.

Figure 4 and 5 show the comparison result of the dimensionless contact load $P/P_C$ and contact area $A/A_C$, evaluated by the different mesh refinement density.

The dimensionless contact loads evaluated by these six mesh density at dimensionless interferences ($\omega \le \omega_c$) were shown in Figure 4. They were not significantly difference between the magnitudes predicted by various mesh density FE model and those of the Hertz theory. Comparison between them showed a constant proportion ratio less than 1%.

Figure 5 showed the dimensionless contact areas evaluated by various mesh density at dimensionless interferences ($\omega \le \omega_c$). The coarser meshes in the mesh refinement level = 1 to level = 3 cause the curves of contact area to be zigzag, whereas the finer meshes in the refinement level = 4 and level = 5 cause the curves to be more smooth,. As the mesh density becomes sufficiently large., the dimensionless contact area indicated a linear relationship with the dimensionless interference.. When mesh refinement was level = 5 and level = 2, the dimensionless contact area showed a very small difference with Hertz theory in the elastic regime, the difference ratio was less than 5%.The meshed model with refinement level = 5 and level = 2 was applied to the elastic-plastic contact analysis.

For tangential contact characteristics of the single asperity, the normal displacement load was applied at first the pilot node of the finite element model of the rigid flat, so the finite element model of the asperity will occurs the elastic-plastic deformation. then the asperity hold the deformation state, a tangential force was applied to the pilot node, the rigid flat will move in the tangential orientation in the form of the micro-displacement. so the relationship between the tangential force and the tangential micro-displacement under different deformation stages of the asperity can be obtained. In the analysis, a

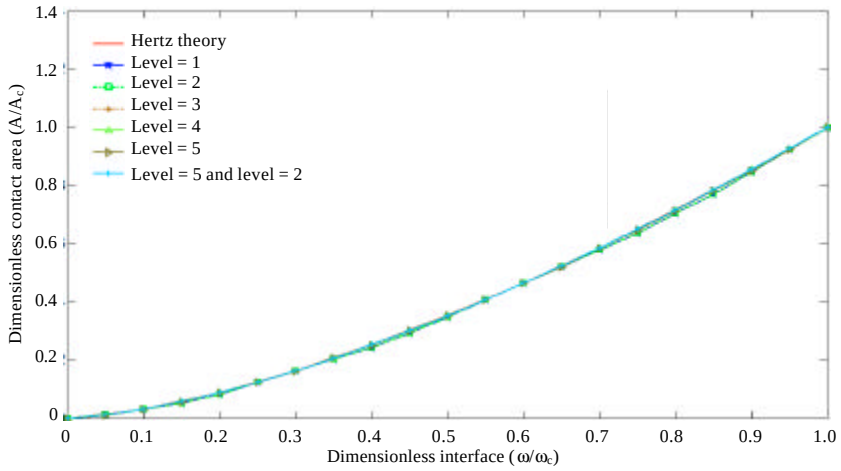


Fig. 4: Comparision of contact load between FEA and Hertz solution

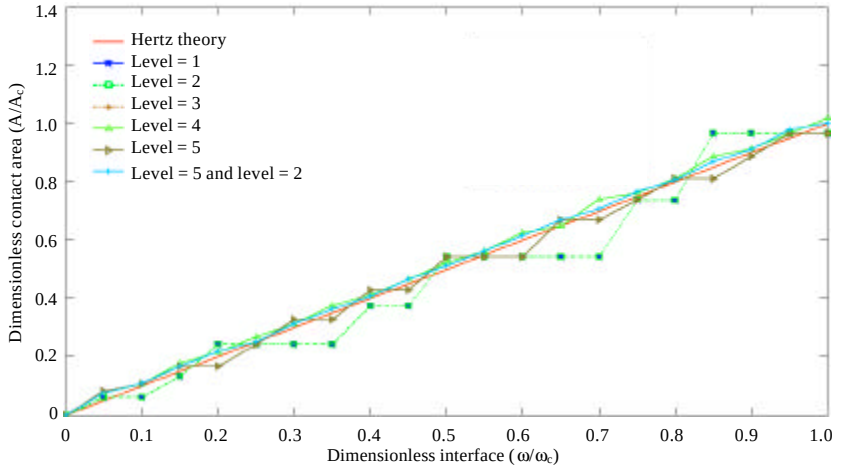


Fig. 5: Comparison of contact area between FEA and Hertz solution

bilinear material property is provided for the deformable asperity, to study the effect of the strain hardening, the different values of tangent modulus $E_T$ are taken, the values range of tangent modulus is between (0~0.02)*E, where E is the asperity materials Young's modulus. The asperity is the elastic perfectly plastic material when $E_T = 0$. In order to make the rigid flat occurs micro-displacement on the surface of asperity when tangential force acts on the pilot node, the friction force will be existed, the coefficient of friction of the asperity material is set to $\mu = 0.3$. then the tangential force required to satisfy following condition:

$$P_{Tmax} = \mu P \quad (8)$$

where, P is the normal force, $P_{Tmax}$ is the maximal tangential force.

## RESULT AND DISCUSSION

Effect of the tangent modulus of materials on the normal contact area and contact force under different normal displacement load are shown in Fig. 6 and 7.

Figure 6 shows dimensionless contact load under different normal displacement load for different tangent modulus. The plot shows a nonlinear feature in between the load and contact interference when the asperity are in the elastic-plastic and fully plastic region. Similar nonlinear feature has been found in between dimensionless contact area and the contact interference which is shown in Fig. 7and 6 shows that the contact load significantly increased as the tangent modulus increase. Figure 7 shows the contact area reducing when the tangent modulus increasing.

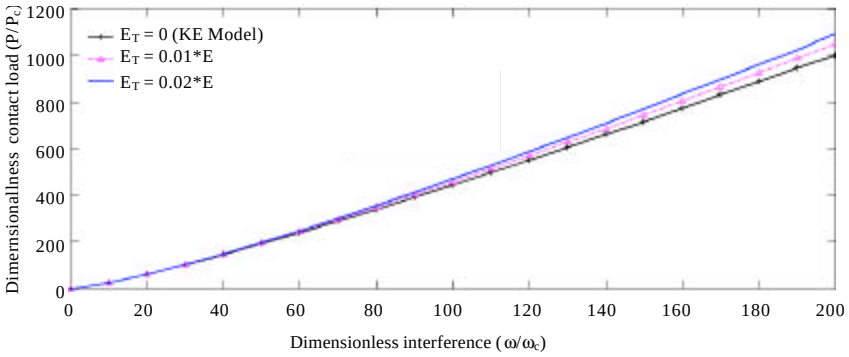


Fig. 6: Comparison of the contact load

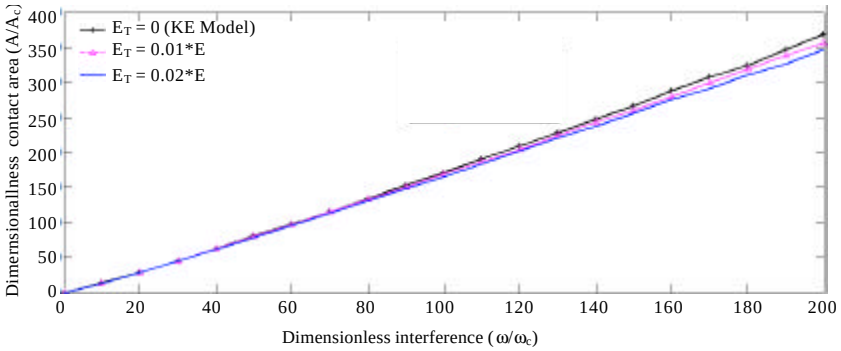


Fig. 7: Comparison of the contact area

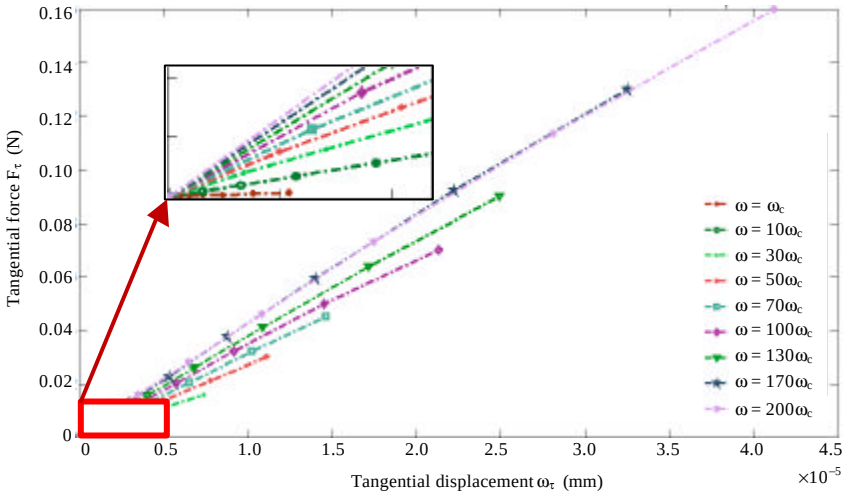


Fig. 8: The relationship between tangential force and tangential displacement ($E_T = 0$)

The relationship of the tangential force and the tangential displacement are shown in the Fig. 8-10 when the asperity is in different elastic-plastic deformation state.

Figure 8-10 shows that the relationship between tangential force and the tangential displacement presents a good linear characteristics, the slope of the linear characteristic is gradually increased as the normal contact displacement increasing. Tangential contact stiffness is defined as the ratio of the tangential force and the tangential micro-displacement, Without loss of generality, the dimensionless tangential contact stiffness is defined

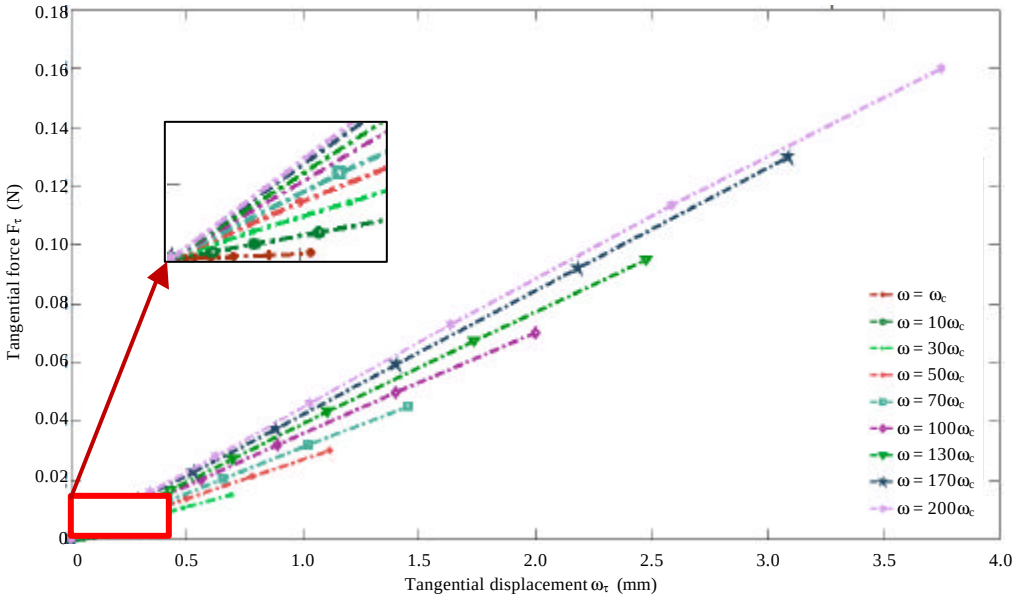


Fig. 9: The relationship between tangential force and tangential displacement ($E_T$ = 0.01E)

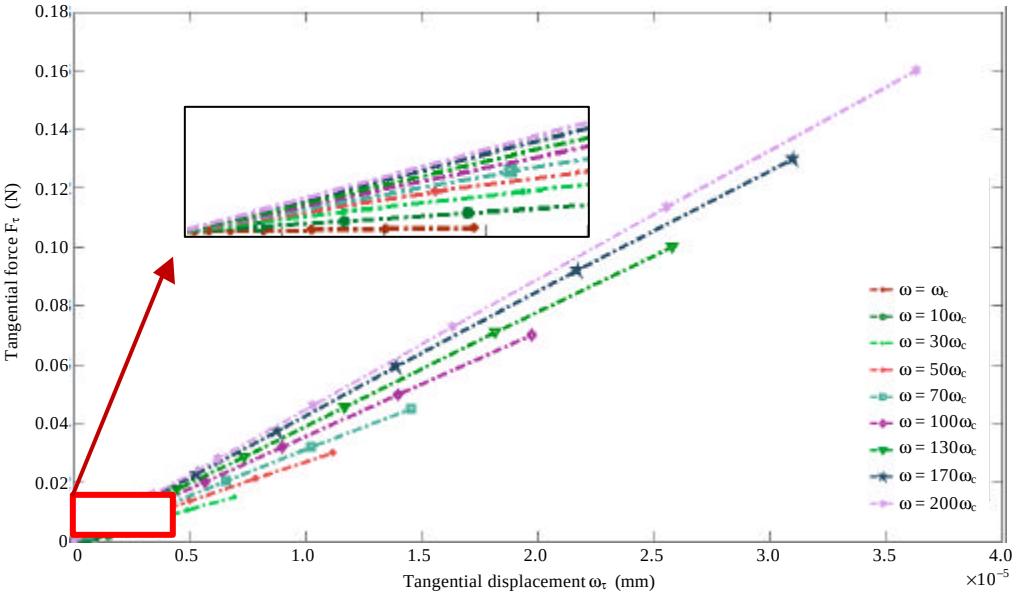


Fig. 10: The relationship between tangential force and tangential displacement ($E_T$ = 0.02E)

as the ratio of actual contact stiffness divided by critical normal contact stiffness, then the comparison of between dimensionless tangential contact stiffness under different tangent modulus is shown in Fig. 11, the result shows that in the range of about $0 \le \frac{\omega}{\omega_c} \le 70$, tangent modulus has not obviously effect on the tangential contact stiffness; In the range of about $\frac{\omega}{\omega_c} > 70$, tangential contact stiffness increasing with the tangent modulus increasing.

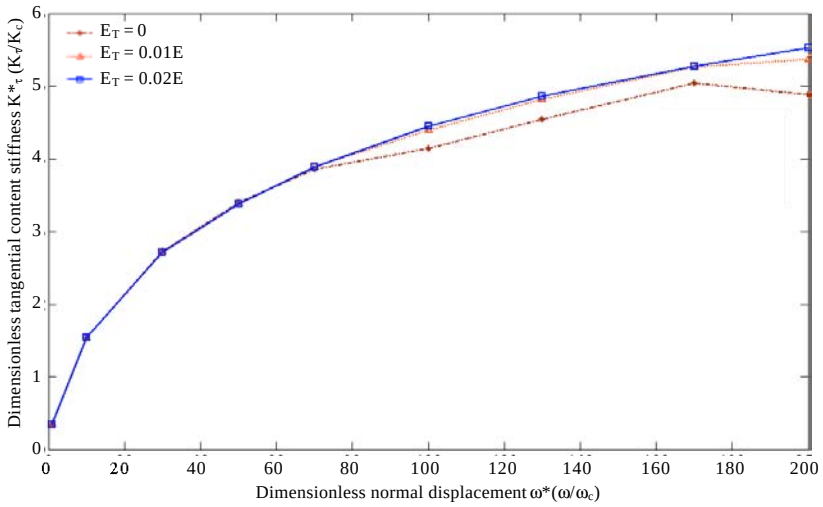


Fig. 11: Comparison between tangential contact stiffness

## CONCLUSION

From the above analysis, we can draw a conclusion that for the precise analysis of finite element model, local mesh refinement method can significantly reduce the number of finite elements, but not affect the accuracy of the analysis results. For the tangential contact characteristic, when in the different normal elastic-plastic deformation state of the asperity, when the rigid flat micro-displacement occurs linear relationship can be obtained between tangential force and tangential displacement. Tangent modulus have a significant impact on the tangential contact stiffness.

The current study only reveals the relationship between the tangential static force and the tangential micro-displacement, but tangential stress distribution on the surface of the asperity, the changes of plastic strain energy, and a dynamic force applied to the asperity are all be in-depth researched.

## ACKNOWLEDGMENT

This study was supported by the National Natural Science Foundation of China(Grant No.51079118 and No. 50275109).

## REFERENCES

Chang, W.R., I. Etsion and D.B. Bogy, 1987. An elastic-plastic model for the contact of rough surfaces. J. Tribol., 109:257–263

Greenwood, J.A. and J.B.P. Williamson, 1966. Contact of nominally flat surfaces. Proc. R. Soc. London Ser. A, 295: 300–319.

Wang, L. and Y. Xiang, 2013. Elastic-plastic contact analysis of a deformable sphere and a rigid flat with friction effect. Adv. Mater. Res., 644:151-156

Kogut, L. and I. Etsion, 2002. Elastic-plastic contact analysis of a sphere and a rigid flat. J. Applied Mech., 69: 657-662

Vu-Quoc, L., X. Zhang and L. Lesburg, 2001. Normal and tangential force-displacement relations for frictional elasto-plastic contact of sphere. Int. J. Solids Struct., 38: 6455-6489

Lin, L.P. and J.F. Lin, 2006. A new method for elastic-plastic contact analysis of a deformable sphere and a rigid flat. J. Tribol., 128:221-229

Sahoo, P., B. Chatterjee and D. Adhikary, 2010. Finite element based elastic-plastic contact behavior of a sphere against a rigid flat-effect of strain hardening. Int. J. Eng. Technol., 21: 1-6

Timoshenko, S. and J.N. Goodier, 1951. Theory of Elasticity. McGraw-Hill Book Co. Inc., New York

Jia, W., C. Yin, F. Yong, D. Cao and H. Yang, 2012. Research on clearance flow of microscopic surface influence. Int. J. Digital Content Technol. Appl., 3: 117-125

Zhao, Y.M., D.M. Maietta and L. Chang, 2000. An asperity microcontact model incorporating the transition from elastic deformation to fully plastic flow. J. Tribol., 122: 86-93

Chen, Z., 2012. Taylor series multipole BEM for 3D elastic contact problems with friction. Int. J. Adv. Comput. Technol., 4: 1-7